

Manganous heteropolytungstates. Synthesis and heteroatom effects in Wells–Dawson-derived sandwich complexes

Israel Martyr Mbomekalle,^a Bineta Keita,^a Louis Nadjo,^{*a} Patrick Berthet,^b Wade A. Neiwert,^c Craig L. Hill,^{*c} Michelle D. Ritorto^c and Travis M. Anderson^c

^a Laboratoire de Chimie Physique, UMR 8000, CNRS, Université Paris-Sud, Bâtiment 420, 91405 Orsay Cedex, France

^b Laboratoire de Physico-Chimie de l'Etat Solide, UMR 8648, CNRS, Université Paris-Sud, Bâtiment 410, 91405 Orsay Cedex, France

^c Department of Chemistry, Emory University, Atlanta, Georgia, 30322

Received 17th April 2003, Accepted 19th May 2003

First published as an Advance Article on the web 6th June 2003

A tetranuclear manganous Wells–Dawson sandwich-type polyoxometalate has been synthesized by the reaction of $\alpha\text{-Na}_{12}(\text{As}_2\text{W}_{15}\text{O}_{56})$ with an aqueous solution of $\text{MnCl}_2 \cdot 4\text{H}_2\text{O}$. The structure of this complex, $\alpha\beta\beta\alpha\text{-Na}_{16}(\text{Mn}^{\text{II}}\text{OH}_2)_2\text{-Mn}^{\text{II}}_2(\text{As}_2\text{W}_{15}\text{O}_{56})_2 \cdot 55\text{H}_2\text{O}$ (**Na1**), was determined by single-crystal X-ray crystallography ($a = 14.5230(12)$ Å, $b = 14.7104(13)$ Å, $c = 19.8927(17)$ Å, $\alpha = 84.326(2)^\circ$, $\beta = 81.709(2)^\circ$, $\gamma = 65.584(2)^\circ$, triclinic, $R_1 = 6.2\%$, based on 26721 independent reflections) and is similar to the phosphorus analogue, $\alpha\beta\beta\alpha\text{-Na}_{16}(\text{Mn}^{\text{II}}\text{OH}_2)_2\text{-Mn}^{\text{II}}_2(\text{P}_2\text{W}_{15}\text{O}_{56})_2$ (**Na2**). Magnetization studies confirm that both **Na1** and **Na2** show antiferromagnetic coupling of the four Mn(II) centers. Despite the structural similarities, electrochemical studies reveal that the presence of arsenic shifts the Mn waves to more positive potentials. Catalytic studies confirm that **1** is a significantly better catalyst than **2** for the H_2O_2 -based epoxidation of *cis*-cyclooctene, cyclohexene, and 1-hexene.

Introduction

The Wells–Dawson-derived sandwich-type polyoxometalates (POMs) are of both practical and intellectual interest.^{1–11} They are comprised of a tetranuclear $[\text{M}_4\text{O}_{14}(\text{OH}_2)_2]$ (where M = Mn(II), Fe(III), Co(II), Ni(II), Cu(II), Zn(II), or Cd(II)) cluster encapsulated by two trivacant $\alpha\text{-X}_2\text{W}_{15}\text{O}_{56}^{12-}$ (where X = P(v) or As(v)) moieties (Fig. 1). The $[\text{M}_4\text{O}_{14}(\text{OH}_2)_2]$ unit has rendered these complexes useful for applications in catalysis^{12–17} and materials chemistry.^{18–20} Concurrently, the $[\text{M}_4\text{O}_{14}(\text{OH}_2)_2]$ cluster is also interesting from an electrochemical perspective since the accumulation of multiple adjacent transition metal cationic centers in the polyoxometalate framework can promote simultaneous multi-electron transfer reactions.^{11,21–29} Typically these reactions proceed by a series of single-electron steps in a potential domain useful for electrocatalysis.^{30–35}

We now report the synthesis of $\alpha\beta\beta\alpha\text{-}(\text{Mn}^{\text{II}}\text{OH}_2)_2(\text{Mn}^{\text{II}})_2\text{-}(\text{As}_2\text{W}_{15}\text{O}_{56})_2^{16-}$ (**Na1**), along with full spectroscopic and solid state characterization. The phosphorus analogue of this complex $\alpha\beta\beta\alpha\text{-}(\text{Mn}^{\text{II}}\text{OH}_2)_2(\text{Mn}^{\text{II}})_2(\text{P}_2\text{W}_{15}\text{O}_{56})_2^{16-}$, (**Na2**) was originally reported by Coronado and co-workers.⁵ This complex has a P atom located in the central tetrahedral heteroatom position rather than an As atom. The As atom is larger than the P atom and has multiple stable oxidation states (As(III) and As(V), for example). Therefore, it can potentially modify both the structural and electronic properties of these sandwich-type complexes. In particular, such modifications of electronic properties could be expected in loose analogy with observations culled from cyclic voltammograms of $\alpha\text{-X}_2\text{MW}_{17}\text{O}_{61}$ derivatives (X = P(v) or As(v)): in these monosubstituted complexes, the presence of As(v) instead of P(v) shifts the entire voltammetric pattern, including the substituent waves, in the positive potential direction.²⁸ A comparison of the X-ray crystal structures of **Na1** and **Na2** reveals that the two complexes have similar bond lengths and angles, with the important exception that the As–O bond lengths are slightly longer than the analogous P–O bond lengths. Cyclic voltammograms, however, reveal that the single Mn wave observed between -0.5 and $+1.6$ V for the two complexes is shifted to a more positive potential by the presence of the As heteroatoms ($+1.142$ V for **Na1** versus $+1.100$ V for **Na2**). In addition, a comparison of the catalytic activity of the two complexes for the H_2O_2 -based epoxidation of alkenes reveals that **1** is significantly more active than **2** under otherwise identical conditions.

Results and discussion

Synthesis and electrochemical characterization of $\alpha\beta\beta\alpha\text{-}(\text{Mn}^{\text{II}}\text{OH}_2)_2\text{-Mn}^{\text{II}}_2(\text{As}_2\text{W}_{15}\text{O}_{56})_2^{16-}$

The procedure used here to synthesize $\alpha\beta\beta\alpha\text{-Na}_{16}(\text{Mn}^{\text{II}}\text{OH}_2)_2\text{-Mn}^{\text{II}}_2(\text{As}_2\text{W}_{15}\text{O}_{56})_2$ (**Na1**) in high yield (ca. 65%) and high purity was adapted from the preparation of the phosphorus analogue $\alpha\beta\beta\alpha\text{-Na}_{16}(\text{Mn}^{\text{II}}\text{OH}_2)_2\text{-Mn}^{\text{II}}_2(\text{P}_2\text{W}_{15}\text{O}_{56})_2$ (**Na2**) with two modifications.⁵ First, $\alpha\text{-As}_2\text{W}_{15}\text{O}_{56}^{12-}$ was used instead of $\alpha\text{-P}_2\text{W}_{15}\text{O}_{56}^{12-}$. Second, the mixture of $\alpha\text{-As}_2\text{W}_{15}\text{O}_{56}$ and Mn(II) was heated at a slightly higher temperature (60 versus 50 °C).

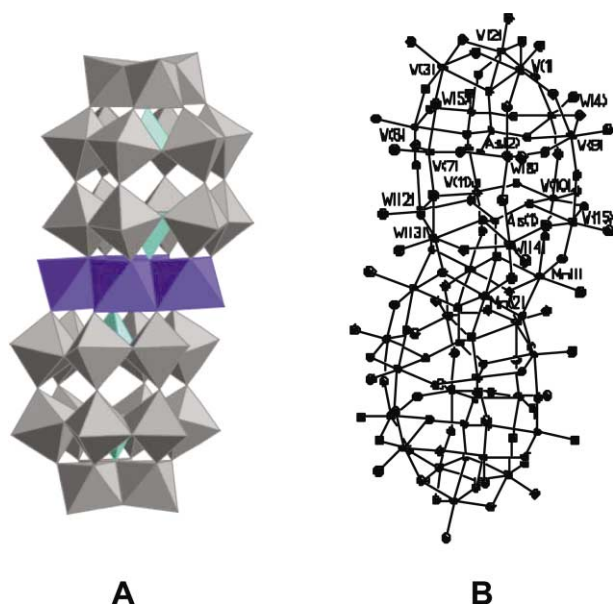


Fig. 1 (A) Polyhedral representation of $\alpha\beta\beta\alpha\text{-}(\text{Mn}^{\text{II}}\text{OH}_2)_2\text{-Mn}^{\text{II}}_2\text{-}(\text{As}_2\text{W}_{15}\text{O}_{56})_2^{16-}$ (**Na1**). (B) Thermal ellipsoid plot (50% probability surfaces) of **Na1**.

DOI: 10.1039/b304255c

This procedure can be modified to use only water as the solvent rather than a 1 M NaCl solution by substituting $\text{Mn}(\text{NO}_3)_2 \cdot 4\text{H}_2\text{O}$ for $\text{MnCl}_2 \cdot 4\text{H}_2\text{O}$. The yield is the same regardless of the solvent used, but the former method seems to give the highest quality crystals.

The synthetic methods used here for Na1 are somewhat different from those recently reported in the literature.¹⁰ First, our methods do not call for the addition of HCl to the medium to obtain a pH value lower than 2. Second, the ratio of excess Mn(II) to $\alpha\text{-As}_2\text{W}_{15}\text{O}_{56}^{12-}$ used is lower than originally reported (1.1 : 1 versus 1.5 : 1). Finally, crystallization was performed at room temperature in our method compared to 5 °C in the original report. Although the original method gives a higher yield (89% versus 65% here), the revised method was essential to growing crystals suitable for a crystallographic study.

The electrochemistry of the W-based waves of Na1 was previously described in a pH = 4 medium.¹⁰ In the pH = 3 medium used here (and in the negative potential domain), there are three W-based waves observed with their reduction peak potentials located at -0.432, -0.540, and -0.760 V (vs. SCE), respectively. As a complement to this data, Fig. 2 shows the main characteristics of the oxidation of the Mn(II) centers of Na1 in a pH = 3 buffer solution. The key feature is the observation of a single step for the simultaneous oxidation of all four Mn(II) centers with the peak potential located at +1.144 V (vs. SCE). The sharpness of the reduction wave and the current crossing upon reversal of the potential collectively indicate the presence of a surface-active species. Fig. 2 also includes data for the phosphorus analogue Na2. The single Mn wave, observed for both complexes, is shifted by 0.042 V to a more positive potential in Na1 by the presence of the As heteroatom.

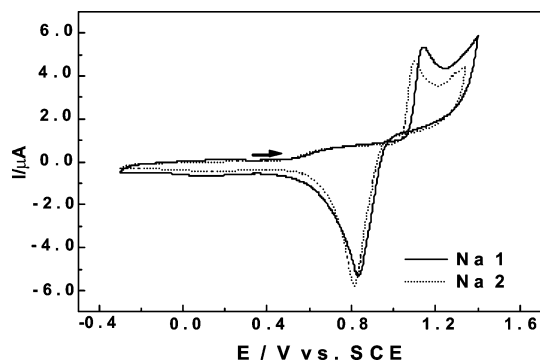


Fig. 2 Cyclic voltammograms of Na1 (solid line) and Na2 (dotted line) (2×10^{-4} M) in a pH = 3 buffer solution (0.5 M Na_2SO_4 and H_2SO_4). The scan rate was 10 mV s^{-1} , the working electrode was glassy carbon, and the reference electrode was SCE. The potential domain was restricted to observe only the Mn(II) centers.

Solid state characterization of $\alpha\beta\beta\alpha\text{-(Mn}^{\text{II}}\text{OH}_2)_2\text{Mn}^{\text{II}}_2\text{-(As}_2\text{W}_{15}\text{O}_{56})_2^{16-}$

The X-ray crystal structure of Na1 is shown in Fig. 1 in both polyhedral and ball-and-stick notation, and a comparison of selected bond lengths and angles are given in Table 1. Like previous reports, the central $[\text{Mn}^{\text{II}}_4\text{O}_{14}(\text{H}_2\text{O})_2]$ unit is sandwiched between two $\alpha\text{-As}_2\text{W}_{15}\text{O}_{56}^{12-}$ moieties.^{3-6,10,11} Bond valence sum (BVS) calculations from the X-ray structure of Na1 yields average oxidation states of 2.17 ± 0.01 and 2.24 ± 0.01 for the two Mn sites (Mn1 and Mn2), respectively.³⁶ Despite the usual difficulty in locating the countercations in POM structures, all 16 Na^+ atoms were located in this structure, and the results are consistent with elemental analysis.

Recently, the structural features of $\alpha\beta\beta\alpha\text{-(Cu}^{\text{II}}\text{OH}_2)_2\text{Cu}^{\text{II}}_2\text{-(As}_2\text{W}_{15}\text{O}_{56})_2^{16-}$ were compared with its phosphorus analogue, $\alpha\beta\beta\alpha\text{-(Cu}^{\text{II}}\text{OH}_2)_2\text{Cu}^{\text{II}}_2\text{(P}_2\text{W}_{15}\text{O}_{56})_2^{16-}$.¹⁰ Four main differences were attributed to the presence of the larger As heteroatom (radius of 0.335 Å for As versus 0.17 Å for P). First, there was approximately 20% less Jahn–Teller distortion of the central

Table 1 Selected bond lengths (Å) and bond angles (°) for Na1 and Na2^{5a}

| | Na1 | Na2 |
|---|-----------|------------------------|
| W–O _t | 1.722(9) | 1.71(2) |
| W–O _b | 1.919(9) | 1.90(2) |
| W–O _c | 2.230(8) | 2.27(2) |
| W–O _d | 2.330(8) | 2.38(2) |
| X–O _c | 1.680(8) | 1.53(2) |
| X–O _d | 1.705(8) | 1.54(2) |
| X–O _{d'} | 1.695(8) | 1.55(2) |
| Mn1 ⋯ Mn2 | 3.300(3) | 3.288(6) |
| Mn1 ⋯ Mn1A | 5.674(4) | 5.659(7) |
| Mn1 ⋯ Mn2A | 3.312(3) | 3.291(7) |
| Mn2 ⋯ Mn2A | 3.396(4) | 3.352(7) |
| Mn1–O1W | 2.195(10) | 2.24(2) |
| O _t –W–O _b (cap) | 101.4(4) | 101.9(22) ^b |
| O _t –W–O _b (belt) | 98.9(4) | 99.4(29) ^b |
| O _t –W–O _d (cap) | 168.8(4) | 169.1(14) ^b |
| O _t –W–O _c (belt) | 170.5(4) | 171.8(10) ^b |
| O _d –X–O _c | 106.8(4) | 107.0(22) ^b |
| O _d –X–O _c | 109.6(4) | 109.0(5) ^b |
| Mn1 ⋯ Mn2 ⋯ Mn1A | 118.5(1) | 118.7(2) |
| Mn2 ⋯ Mn1 ⋯ Mn2A | 61.9(1) | 61.3(1) |

^a O_t = terminal oxygen; O_b = doubly bridging oxygen; O_c = triply bridging oxygen; O_d = quadruply bridging oxygen; O_{d'} = quadruply bridging oxygen that bonds to the Mn atoms; X = central heteroatom (As(V) in Na1 and P(V) in Na2), ^b uncertainty was unpublished and therefore statistically determined from the random scatter in the data.

Cu(II) atoms in the arsenic compound. Second, the four planar Cu(II) atoms comprising the $[\text{Cu}^{\text{II}}_4\text{O}_{14}(\text{H}_2\text{O})_2]$ unit have shorter Cu ⋯ Cu distances in the arsenic structure (approximately 0.05 Å shorter) compared to the phosphorus analogue. Third, the average distance between the proximal heteroatom (As or P) and each Cu(II) center is longer in the arsenic analogue than in the phosphorus complex. Fourth, the proximal As heteroatom has less deviation from the mean planes of Cu^{II}_4 or W^{VI}_6 compared to the phosphorus complex. A comparison of Na1 with its phosphorus analogue ($\alpha\beta\beta\alpha\text{-(Mn}^{\text{II}}\text{OH}_2)_2\text{Mn}^{\text{II}}_2\text{-(P}_2\text{W}_{15}\text{O}_{56})_2^{16-}$, Na2) reveals that it does not show the pronounced differences observed in the Cu(II) complexes. The As–O bond lengths are slightly longer than the analogous P–O bond lengths, but there is no alteration of the $\alpha\text{-As}_2\text{W}_{15}\text{O}_{56}^{12-}$ framework or the central $[\text{Mn}^{\text{II}}_4\text{O}_{14}(\text{H}_2\text{O})_2]$ unit based on the average bond lengths and angles shown in Table 1. These results suggest that the structure of Na1 should be representative of complexes containing other transition metals which do not show significant Jahn–Teller distortion (*i.e.* $\alpha\beta\beta\alpha\text{-(M}^{\text{II}}\text{OH}_2)_2\text{-M}^{\text{II}}_2\text{(As}_2\text{W}_{15}\text{O}_{56})_2^{16-}$, where M = Zn, Ni, or Co).

The temperature dependence of the magnetization of Na1 and Na2 were studied in a 0.1 T field using a SQUID magnetometer (Quantum Design MPMS-5). The $\chi_m T$ values calculated from these studies, corrected for diamagnetic contributions, are plotted as functions of temperature (*T*) in Fig. 3A. The two samples give very similar data. For temperatures higher than 150 K, the $\chi_m T$ products reach nearly constant values of 17.4 ± 0.2 and $18.2 \pm 0.2 \text{ emu K mol}^{-1}$ for Na1 and Na2, respectively. These values correspond nicely with the theoretical value of $17.5 \text{ emu K mol}^{-1}$ expected for four non-interacting high spin Mn(II) centers. Below 50 K, the $\chi_m T$ values decrease quickly with decreasing temperature. This behavior may be attributed to antiferromagnetic interactions between the Mn(II) ions.

Similar observations were reported by Coronado and co-workers for the analogous phosphorus compound (Na2) with a maximum $\chi_m T$ value of $17.2 \text{ emu K mol}^{-1}$.⁵ These investigators also reported the possible presence of paramagnetic impurities in their sample. This observation could account for the differences observed in Na1 and Na2. An indication of the presence of paramagnetic impurities may be found in the shape of the

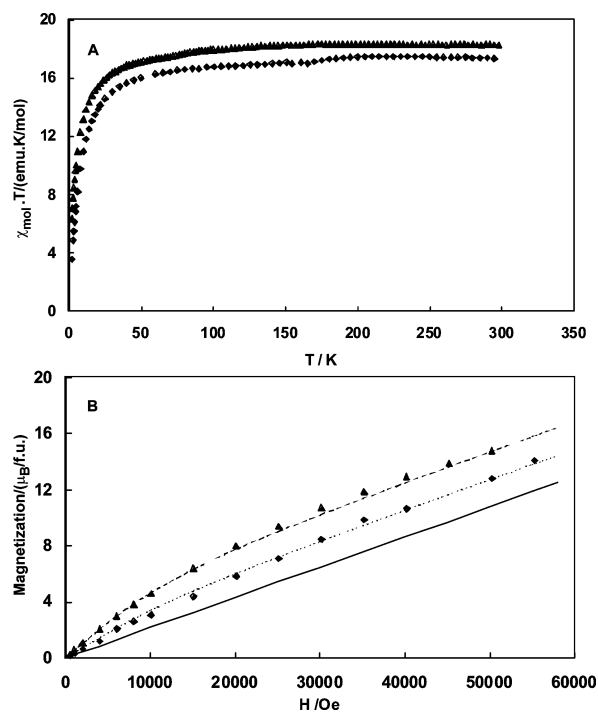


Fig. 3 (A) Plot of $\chi_m(T)$ versus T for Na1 (diamonds) and Na2 (triangles). (B) Plot of magnetization versus H for Na1 (diamonds) and Na2 (triangles). The solid line represents the contribution of the $[\text{Mn}^{\text{II}}_4\text{O}_{14}(\text{H}_2\text{O})_2]$ unit. The sum of this contribution with that of $S = 5/2$ paramagnetic ions (not associated with the POM) is represented by the dotted line ($\lambda = 0.4$) for Na1 and the dashed line ($\lambda = 0.8$) for Na2; λ represents the molar ratio between the paramagnetic ions and the $[\text{Mn}^{\text{II}}_4\text{O}_{14}(\text{H}_2\text{O})_2]$ units.

magnetization ($M(H)$) versus magnetic field curves shown in Fig. 3B. Assuming there is a linear variation of the magnetization of the $[\text{Mn}^{\text{II}}_4\text{O}_{14}(\text{H}_2\text{O})_2]$ unit with the magnetic field, the curves should appear as a sum of both the aforementioned linear contribution and a Brillouin-like contribution coming from the paramagnetic impurity. For a $S = 5/2$ impurity such as Mn(II), the ratio (λ) between the paramagnetic ions not structurally associated with the POM unit and the $[\text{Mn}^{\text{II}}_4\text{O}_{14}(\text{H}_2\text{O})_2]$ clusters may be estimated as 0.4 for Na1 and 0.8 for Na2. The latter value is close to that obtained by Coronado (0.75) on their analysis of Na2.⁵ The exact nature of the paramagnetic impurity is difficult to determine. However, at least two main types of impurities may be considered. First, free (non-POM-associated) Mn(II) ions may be present. Second, decomposition products of Na1 or Na2 may be present such as various mono-, di-, and tri-Mn(II)-substituted POMs including but not limited to $\alpha_1\text{-X}_2(\text{Mn}^{\text{II}}\text{OH}_2)\text{W}_{17}\text{O}_{61}^{8-}$, $\alpha_2\text{-X}_2(\text{Mn}^{\text{II}}\text{OH}_2)\text{W}_{17}\text{O}_{61}^{8-}$, $\alpha\text{-X}_2(\text{Mn}^{\text{II}}\text{OH}_2)_2\text{W}_{16}\text{O}_{60}^{10-}$, or $\alpha\text{-X}_2(\text{Mn}^{\text{II}}\text{OH}_2)_3\text{W}_{15}\text{O}_{59}^{12-}$.^{5,37} The former case is illustrated by a recent observation by Kortz in which one of the five Mn(II) ions in $\text{K}_4\text{MnNa}_6(\text{MnOH}_2)_2\text{Mn}_2(\text{SiW}_9\text{O}_{34})_2 \cdot 33\text{H}_2\text{O}$ is present as a counteranion.^{38,39} In the case of Na1, free Mn(II) ions were not detected by elemental analysis, cyclic voltammetry, or X-ray crystallographic studies. The presence of paramagnetic impurities should lead to some corrections of the experimental $\chi_m T$ values to obtain actual numbers corresponding to the $[\text{Mn}^{\text{II}}_4\text{O}_{14}(\text{H}_2\text{O})_2]$ unit alone. These corrections are not obvious since they depend on the spin value of the magnetic clusters present in the fragments. However, they would primarily reduce the magnetization at low temperatures and thus would not modify the conclusion concerning the antiferromagnetic nature of the interactions inside the $[\text{Mn}^{\text{II}}_4\text{O}_{14}(\text{H}_2\text{O})_2]$ cluster.

Catalytic studies

Table 2 reports the oxidation of three representative alkenes by H_2O_2 catalyzed by **1** or **2** in 1,2-dichloroethane and the distri-

Table 2 Product distributions for ambient temperature oxidation of alkenes by H_2O_2 catalyzed by **1** and **2**^a

| Substrate (Catalyst) | Product Selectivity (TON) ^b | | |
|----------------------|--|----------------|----------------|
| | | | |
| (1) | 99%(1550) | 0 ^c | 0 ^c |
| (2) | 99%(756) | 0 ^c | 0 ^c |
| | | | |
| (1) | 83%(189) | 4%(10) | 12%(28) |
| (2) | 87%(118) | 5%(7) | 6%(16) |
| | | | |
| (1) | 99%(53) | 0 ^c | 0 ^c |
| (2) | 99%(39) | 0 ^c | 0 ^c |

^a Conditions: 68 μL of 30% H_2O_2 was injected into 1 mL of POM stock solution (containing 0.2 μmol of POM) and 1.0 mmol alkene substrate under Ar to initiate the reaction. Organic products were identified and quantified by GC/MS and GC. ^b Selectivity = (moles of indicated product/moles of all organic products derived from the substrate) $\times 100$ (TON = moles of indicated product/moles of catalyst after 24 h). ^c No products within the detection limit ($<0.2\%$).

bution of alkene-derived oxidation products at room temperature. Manganese-containing polyoxometalates have been the focus of a number of catalytic studies since the discovery that $\text{WZn}(\text{MnOH}_2)_2(\text{ZnW}_9\text{O}_{34})^{12-}$ is an oxidatively and solvolytically stable catalyst for the oxidation of various organic substrates with both high selectivity ($>99\%$) and high turnover numbers (hundreds to thousands of turnovers) in biphasic (aqueous-organic) systems.^{40,41} While the $\text{WZn}(\text{Mn}^{\text{II}}\text{OH}_2)_2(\text{ZnW}_9\text{O}_{34})^{12-}$ complex was the most active catalyst reported in these studies, the related sandwich-type complex, $(\text{Mn}^{\text{II}}_2)(\text{Mn}^{\text{II}}\text{OH}_2)_2(\text{PW}_9\text{O}_{34})^{10-}$, was completely inactive.^{41a,b} Although both **1** and **2** have the same $[\text{Mn}^{\text{II}}_4\text{O}_{14}(\text{H}_2\text{O})_2]$ unit as $(\text{Mn}^{\text{II}}_2)(\text{Mn}^{\text{II}}\text{OH}_2)_2(\text{PW}_9\text{O}_{34})^{10-}$, these complexes show considerable activity under similar conditions. Remarkably, the arsenic complex, **1**, is consistently more active than the structurally analogous complex, **2**, for all three substrates examined. In the case of *cis*-cyclooctene, for example, **1** gives more than double the number of turnovers observed for **2** under identical conditions, without a loss of selectivity. Yields based on H_2O_2 consumption are low in all reactions, however, suggesting that there is some disproportionation of H_2O_2 . Interestingly, for all three substrates the same final concentration of H_2O_2 was observed for both catalysts after 24 h, suggesting that the heteroatoms do not play a role in this reaction. Both POMs are stable under catalytic conditions. No decomposition products were observed by FT-IR after a solution of the POM, alkene, and 68 μL of 30% aqueous H_2O_2 were incubated for 24 h.

Experimental

General methods and materials

$\alpha\text{-Na}_{12}(\text{As}_2\text{W}_{15}\text{O}_{56})$ and $\alpha\beta\beta\alpha\text{-(Mn}^{\text{II}}\text{OH}_2)_2(\text{Mn}^{\text{II}})_2(\text{P}_2\text{W}_{15}\text{O}_{56})_2^{16-}$ were obtained by published procedures,^{5,10} and purity was confirmed by IR and cyclic voltammetry. Elemental analyses of As, Mn, and Na were performed by Kanti Labs (Mississauga, Canada). Quantitative analysis of W was performed in our laboratory by a modified literature method.⁴² Infrared spectra (1% sample in KBr) were recorded on a Perkin Elmer Spectrum One FT-IR instrument. All electrochemical measurements were performed with an EG and G 273A apparatus under computer control (M270 software). Potentials are quoted against a saturated calomel electrode (SCE). Magnetic measurements were

carried out on polycrystalline samples using a SQUID magnetometer, Quantum Design MPMS-5. Organic products were quantified using a Hewlett-Packard 6890 gas chromatograph fitted with a flame ionization detector, a 5% phenyl methyl silicone capillary column, and a Hewlett-Packard 6890 series integrator (with N₂ carrier gas).

Synthesis of $\alpha\beta\beta\alpha$ -Na₁₆(Mn^{II}OH)₂Mn^{II}(As₂W₁₅O₅₆)₂·55H₂O (Na1)

A 0.44 g (2.2 mmol) sample of MnCl₂·4H₂O (or 0.55 g of Mn(NO₃)₂·4H₂O) was dissolved in 50 mL of 1 M NaCl solution (de-ionized water was used with Mn(NO₃)₂·4H₂O) and 4.5 g (1 mmol) of solid α -Na₁₂(As₂W₁₅O₅₆) was added in small portions with continuous stirring of the solution. The orange suspension was heated at 60 °C in a water bath until complete dissolution of the solid was achieved, and the clear solution was filtered hot. The orange microcrystalline solid that forms upon slow cooling was re-crystallized from 20 mL of deionized water. Diffraction-quality crystals formed upon standing (yield 65%). Thermogravimetric analysis of the sample (with heating up to 500 °C) corresponds to a loss of 55 water molecules per molecule of Na1. IR (1% KBr pellet, 1300–400 cm⁻¹): 943 (s), 902 (sh), 871 (m), 824 (m), 764 (m), and 715 (m). Anal. Calcd for H₁₁₀As₄Mn₄Na₁₆O₁₆₈W₃₀: As, 3.26; Mn, 2.39; Na, 4.01; W, 60.05. Found: As, 3.32; Mn, 2.42; Na, 4.11; W, 60.2%. [MW = 9185.]

X-ray crystallography

A suitable crystal of Na1 was coated with Paratone N oil, suspended on a small fiber loop, and placed in a stream of cooled nitrogen (100 K) on a Bruker D8 SMART APEX CCD sealed tube diffractometer with graphite monochromated Mo K α (0.71073 Å) radiation. A sphere of data was measured using combinations of ϕ and ω scans with 10 s frame exposures and 0.3° frame widths. Data collection, indexing, and initial cell refinements were carried out using SMART software.⁴³ Frame integration and final cell refinements were carried out using SAINT software.⁴⁴ The final cell parameters were determined from least-squares refinement. A multiple absorption correction for each data set was applied using the program SADABS.⁴⁵ The structure was solved using direct methods and difference Fourier techniques.⁴⁶ All Mn, As, Na, and W atoms were refined anisotropically. Of the 172 O atoms found, 114 atoms are associated with the POM structure itself (112 as oxo anions and two as axial water ligands on Mn(1) and Mn(1a)) and 58 atoms are solvent (water) molecules. No H atoms associated with the water molecules were located in the difference Fourier map. The residual electron density (largest difference peak of 6.51 e⁻ Å⁻³) was located 0.63 Å from W(14). The final R₁ scattering factors and anomalous dispersion corrections were taken from the *International Tables for X-ray Crystallography*.⁴⁷ Structure solution, refinement, graphics, and generation of publication materials were performed using SHELXTL, V5.10 software. Additional details are given in Table 3 and a thermal ellipsoid plot (at the 50% probability level) is given in Fig. 1B.

CCDC reference number 208670.

See <http://www.rsc.org/suppdata/dt/b3/b304255c/> for crystallographic data in CIF or other electronic format.

Catalysis

Stock solutions were prepared by mixing 0.01 mmol of the POM (Na1 or Na2) with 1 mmol of methyltricaprylammonium chloride in 50 mL of 1,2-dichloroethane and filtering off the precipitated NaCl. In a typical reaction, the alkene substrate (1.0 mmol) and 1 mL of the POM stock solution (containing 0.2 μmol of POM) were stirred under Ar at 25 °C (with 3.0 μL decane) in a sealed vial. The reaction was initiated by the

Table 3 Crystal data and structure refinement for Na1

| | |
|--|--|
| Empirical formula | As ₄ H ₁₂₀ Mn ₄ Na ₁₆ O ₁₇₂ W ₃₀ |
| Formula weight | 9275.74 |
| Crystal system | Triclinic |
| Space group | P $\bar{1}$ |
| <i>a</i> , <i>b</i> , <i>c</i> /Å | 14.5230(12), 14.7104(13), 19.8927(17) |
| <i>a</i> , <i>β</i> , <i>γ</i> /° | 84.326(2), 81.709(2), 65.584(2) |
| <i>Z</i> | 1 |
| Absorption coefficient/mm ⁻¹ | 23.799 |
| Reflections collected | 66374 |
| Independent reflections | 26721 |
| GOF on <i>F</i> ² | 1.052 |
| Final <i>R</i> ₁ ^a [<i>R</i> > 2σ(<i>I</i>)] | 0.0620 |
| Final <i>wR</i> ₂ ^b [<i>R</i> > 2σ(<i>I</i>)] | 0.1428 |

$$^a R_1 = \sum |F_o - |F_c|| / \sum |F_o|. \quad ^b wR_2 = \{ \sum [w(F_o^2 - F_c^2)] / \sum [w(F_o^2)] \}^{0.5}.$$

addition of 68 μL of 30% aqueous H₂O₂. The organic products were identified and quantified by GC, using decane as the internal standard. The final H₂O₂ concentration was measured using standard iodometric analyses.⁴⁸

Acknowledgements

This work was supported in part by the University Paris XI and the CNRS (UMR 8000 and 8648). We also thank the NSF Grant CHE-9975453 for the research, Grant CHE-9974864 for funding the D8 X-ray instrument, and Kenneth I. Hardcastle for assistance with X-ray crystallography.

References and Notes

- R. G. Finke and M. W. Droegge, *Inorg. Chem.*, 1983, **22**, 1006–1008.
- R. G. Finke, M. W. Droegge and P. J. Domaille, *Inorg. Chem.*, 1987, **26**, 3886–3896.
- T. J. R. Weakley and R. G. Finke, *Inorg. Chem.*, 1990, **29**, 1235–1241.
- R. G. Finke and T. J. R. Weakley, *J. Chem. Crystallogr.*, 1994, **24**, 123–128.
- C. J. Gómez-García, J. J. Borrás-Almenar, E. Coronado and L. Ouahab, *Inorg. Chem.*, 1994, **33**, 4016–4022.
- X. Zhang, Q. Chen, D. C. Duncan, C. Campana and C. L. Hill, *Inorg. Chem.*, 1997, **36**, 4208–4215.
- X. Zhang, T. M. Anderson, Q. Chen and C. L. Hill, *Inorg. Chem.*, 2001, **40**, 418–419.
- T. M. Anderson, K. I. Hardcastle, N. Okun and C. L. Hill, *Inorg. Chem.*, 2001, **40**, 6418–6425.
- T. M. Anderson, X. Zhang, K. I. Hardcastle and C. L. Hill, *Inorg. Chem.*, 2002, **41**, 2477–2488.
- L. H. Bi, E.-B. Wang, J. Peng, R. D. Huang, L. Xu and C. W. Hu, *Inorg. Chem.*, 2000, **39**, 671–679.
- I. M. Mbomekalle, B. Keita, L. Nadjo, P. Berthet, K. I. Hardcastle, C. L. Hill and T. M. Anderson, *Inorg. Chem.*, 2003, **42**, 1163–1169.
- C. L. Hill and C. M. Prosser-McCartha, *Coord. Chem. Rev.*, 1995, **143**, 407–455.
- T. Okuhara, N. Mizuno and M. Misono, *Adv. Catal.*, 1996, **41**, 113–252.
- N. Mizuno and M. Misono, *Chem. Rev.*, 1998, **98**, 199–218.
- I. V. Kozhevnikov, *Chem. Rev.*, 1998, **98**, 171–198.
- R. Neumann, *Prog. Inorg. Chem.*, 1998, **47**, 317–370.
- D. E. Katsoulis, *Chem. Rev.*, 1998, **98**, 359–388.
- V. W. Day and W. G. Klemperer, *Science*, 1985, **228**, 533–541.
- E. Coronado and C. J. Gómez-García, *Chem. Rev.*, 1998, **98**, 273–296.
- A. Müller, P. Kogerler and C. Kuhlmann, *Chem. Commun.*, 1999, 1347–1358.
- B. Keita and L. Nadjo, *Top. Curr. Electrochem.*, 1993, **2**, 77–106.
- B. Keita, Y. W. Lu, L. Nadjo, R. Contant, M. Abbessi, J. Canny and M. Richet, *J. Electroanal. Chem. Interfacial Electrochem.*, 1999, **477**, 146–157.
- R. Contant, M. Abbessi, J. Canny, M. Richet, B. Keita, A. Belhouari and L. Nadjo, *Eur. J. Inorg. Chem.*, 2000, 567–574.
- R. Contant, M. Abbessi, J. Canny, A. Belhouari, B. Keita and L. Nadjo, *Inorg. Chem.*, 1997, **36**, 4961–4967.
- B. Keita, A. Belhouari, L. Nadjo and R. Contant, *J. Electroanal. Chem.*, 1998, **442**, 49–57 and references therein.
- B. Keita, F. Girard, L. Nadjo, R. Contant, J. Canny and M. Richet, *J. Electroanal. Chem.*, 1999, **478**, 76–82.

- 27 R. Belghiche, R. Contant, Y. W. Lu, B. Keita, M. Abbessi, L. Nadjo and J. Mahuteau, *Eur. J. Inorg. Chem.*, 2002, 1410–1414.
- 28 B. Keita, I. M. Mbomekalle, L. Nadjo and R. Contant, *Eur. J. Inorg. Chem.*, 2002, 473–479.
- 29 B. Keita, I. M. Mbomekalle, L. Nadjo and R. Contant, *Electrochem. Commun.*, 2001, **3**, 267–273.
- 30 B. Keita, A. Belhouari, L. Nadjo and R. Contant, *J. Electroanal. Chem.*, 1995, **181**, 243–250.
- 31 J. E. Toth and F. C. Anson, *J. Am. Chem. Soc.*, 1989, **111**, 2444–2451.
- 32 J. E. Toth and F. C. Anson, *J. Electroanal. Chem.*, 1989, **256**, 361–370.
- 33 B. Keita, K. Essaadi, L. Nadjo, R. Contant and Y. Justum, *J. Electroanal. Chem.*, 1996, **404**, 271–279.
- 34 B. Keita and L. Nadjo, *Mater. Chem. Phys.*, 1989, **22**, 77–103.
- 35 A. Sadakane and E. Steckhan, *Chem. Rev.*, 1998, **98**, 219–237.
- 36 I. D. Brown and D. Altermatt, *Acta Crystallogr., Sect. B*, 1985, **41**, 244–247.
- 37 R. Contant and G. Hervé, *Rev. Inorg. Chem.*, 2002, **22**, 63–111.
- 38 U. Kortz, S. Isber, M. H. Dickman and D. Ravot, *Inorg. Chem.*, 2000, **39**, 2915–2922.
- 39 A similar observation was made by Weakley and Finke, see ref. 3.
- 40 The sandwich-type complex $\text{WZn}(\text{MnOH})_2(\text{ZnW}_9\text{O}_{34})_2^{12-}$ was first prepared by Tourné and co-workers. See C. M. Tourné, G. F. Tourné and F. Zonnevijlle, *J. Chem. Soc., Dalton Trans.*, 1991, 143–155.
- 41 Representative catalytic studies of manganese-containing POMs include: (a) R. Neumann and M. Gara, *J. Am. Chem. Soc.*, 1994, **116**, 5509–5510; (b) R. Neumann and M. Gara, *J. Am. Chem. Soc.*, 1995, **117**, 5066–5074; (c) R. Neumann and A. M. Khenkin, *Chem. Commun.*, 1998, 1967–1968; (d) R. Ben-Daniel, L. Weiner and R. Neumann, *J. Am. Chem. Soc.*, 2002, **124**, 8788–8789; (e) W. Adam, P. L. Alsters, R. Neumann, C. R. Saha-Moller, D. Sloboda-Rozner and R. Zhang, *Synlett.*, 2002, 2011–2014.
- 42 S. Lis and S. But, *J. Alloys Compd.*, 2000, **303–304**, 132–136.
- 43 SMART, version 5.624, Bruker AXS, Inc., Madison, WI, 2002.
- 44 SAINT, version 6.36A, Bruker AXS, Inc., Madison, WI, 2002.
- 45 G. Sheldrick, SADABS, version 2.03, University of Göttingen, Göttingen, Germany, 2001.
- 46 SHELXTL, version 6.12, Bruker AXS, Inc., Madison, WI, 2002.
- 47 *International Tables for X-ray Crystallography*, Kynoch Academic Publishers, Dordrecht, Netherlands, 1992, vol. C.
- 48 R. A. Day, Jr. and A. L. Underwood, *Quantitative Analysis*, Prentice-Hall, Englewood Cliffs, NJ, 5th edn., 1986.